

## Porosity Determination by Pulsed Thermography in Reflection Mode

by G. Mayr\* and G. Hendorfer\*\*

\*Research & Development Ltd., University of Applied Sciences, Wels (Austria), [g.mayr@fh-wels.at](mailto:g.mayr@fh-wels.at)

\*\*Upper Austrian University of Applied Sciences, Wels (Austria), [g.hendorfer@fh-wels.at](mailto:g.hendorfer@fh-wels.at)

### Abstract

In this work we measure the thermal diffusivity of a series of porous carbon fibre reinforced plastics specimens using pulsed thermography in reflection mode. These diffusivity values are compared with porosity values derived by means of computed tomography. In addition, numerical simulations of the heat transfer are performed using a finite-element program. The simulation shows that the effective thermal diffusivity values derived in reflection mode scatter more than the transmission results especially at low porosity. Furthermore, for porosities higher than 10 percent the sensitivity for both methods decreases. The experimental results are similar to those seen in the numerical study.

### 1. Introduction

Active thermography offers a rapid, non-contact and non-destructive testing technique, which can be used to find buried discontinuities in materials [1]. These discontinuities such as the porosity in carbon fibre reinforced plastics (CFRP) have a strong effect on a material's physical and mechanical properties. An increase in porosity leads to a decrease in density, modulus and the strength of the composite. As the porosity increases above 0.9 % the interlaminar shear strength decreases significantly in CFRP [2]. For example, the interlaminar shear strength of CFRP decreases by about 7 % per 1 % porosity, up to a total porosity level of 4 % [3]. The porosity  $\Phi$  is defined as the volume of pores  $V_p$  over the total volume of the material and voids  $V$  by following equation  $\Phi = V_p / V$ .

In the aerospace industry a porosity level of 2.5 % has become the general level of acceptance for most safety-critical CFRP components. Pulsed thermography, i.e. thermal diffusivity imaging, has the potential to detect and quantify such porosities [4, 5]. The first studies from Connolly, Heath and Winfree showed the correlation between thermal diffusivity and porosity. Furthermore Zalameda and Winfree characterized simulated porosities in composites using lock-in techniques to calculate the thermal diffusivity [6]. Other qualitative studies have demonstrated that there is a good agreement between ultrasonic and pulsed thermography when testing real CFRP structures on porosity [7]. Moreover, Ringermacher [8] and Torquato [9] have developed a model for predicting the thermal diffusivity of a two phase material with elliptically shaped inclusions. In a former work [10] we validated this model based on measurements by means of pulsed thermography and X-ray computed tomography (CT). However, all these studies were carried out in transmission mode and so there is a lack of knowledge on the subject of how these results can be compared to measurements made in reflection mode.

The aim of this study is to investigate the dependency of thermal diffusivity on porosity. The experiments are done by means of pulsed thermography in reflection mode. The alignment of the infrared source and detector in the reflection mode of a thermography setup offers the possibility of testing complex shaped structures, where the common transmission mode is not applicable, i.e. CFRP honeycomb sandwich panels. Reference experiments for thermography were performed by means of CT to investigate the absolute volume porosity, distribution and dimension of the pores. In addition to the experiments, two dimensional (2D) numerical simulations of the heat transfer were performed using a finite-element program.

### 2. Theory

The heating and cooling down process during a pulsed thermography experiment for porous materials can be described as follows

$$\rho(x, y, z)C_p(x, y, z)\frac{\partial T(t, x, y, z)}{\partial t} = \nabla(k(x, y, z)\nabla T(t, x, y, z)) \quad (1)$$

where  $\rho$  is the material density,  $C_p$  the specific heat capacity,  $k$  the heat conductivity,  $T$  the temperature,  $t$  the time and  $x, y, z$  the spatial coordinates. The coefficients in the three dimensional partial differential equation are functions in space which have jump discontinuities at the boundary of the pore to the matrix. For this formulation of the problem no simple analytical solution  $T(t,x,y,z)$  exists.

However, Kerrisk [11] introduced a criterion by which the material under investigation can be considered homogeneously under transient conditions. The validity of this criterion can be expressed by the following equation:

$$\frac{d}{\phi^{-1/3}} < \frac{L}{M} \text{ with } 100 < M < 1000 \quad (2)$$

where  $d$  is the averaged pore diameter and  $L$  the thickness of the specimen. If this criterion is fulfilled the concept of "effective parameters" can be used. "Effective parameters" are properties of an equivalent homogeneous material, which produce the same physical effects as a heterogeneous material. In the case of porous CFRP the average spacing between the pores is much smaller than the thickness of the specimen. Furthermore, the homogeneous heating and the simple plate geometry of the test specimens allows a one dimensional modelling. Thus, the following partial differential equation is an appropriately simple model, which can be used instead of Eq. (1):

$$\frac{1}{\alpha} \frac{\partial T}{\partial t} = \frac{\partial^2 T}{\partial z^2} \quad (3)$$

To calculate the effective thermal diffusivity  $\alpha = k/(\rho \cdot C_p)$  the following two solutions of the Fourier equation (Eq. 3) for the adiabatic heating of a thermally thick specimen under the assumption of a dirac-like excitation are used [12]:

$$T(t, z) = T_0 + \frac{W}{\rho C_p \sqrt{\pi \alpha t}} \exp\left(-\frac{z^2}{4 \alpha t}\right) \quad (4)$$

and

$$T(t, 0) = T_0 + \frac{W}{e \sqrt{\pi t}} \quad (5)$$

where  $T_0$  is the initial temperature,  $W$  is the absorbed heat energy per unit area and  $e$  the thermal effusivity, defined as  $e = (k \cdot \rho \cdot C_p)^{1/2}$ . These equations describe the instantaneous pulse-heating of a material as we have in pulsed thermography experiments. Based on these solutions two procedures are applied to calculate the effective thermal diffusivity. The procedures for transmission (LDF) [13] and reflection mode (TSR) [14] are independent of local changes in illumination, surface absorption or local thermal emission coefficients. In figure 1 the determination of the characteristic parameters  $\beta$  and  $t^*$  are shown.

The determination of the parameters  $\beta$  and  $t^*$  allow a calculation of the observation time  $t_o$  as follows

$$t_o = \frac{L^2}{\alpha} = \pi \cdot t^* = 4 \cdot \beta \quad (6)$$

Knowledge of the thickness  $L$  is required to calculate the effective thermal diffusivity from the observation time. By these methods the thermal diffusivity can be obtained as a quantity averaged over the specimen's thickness.

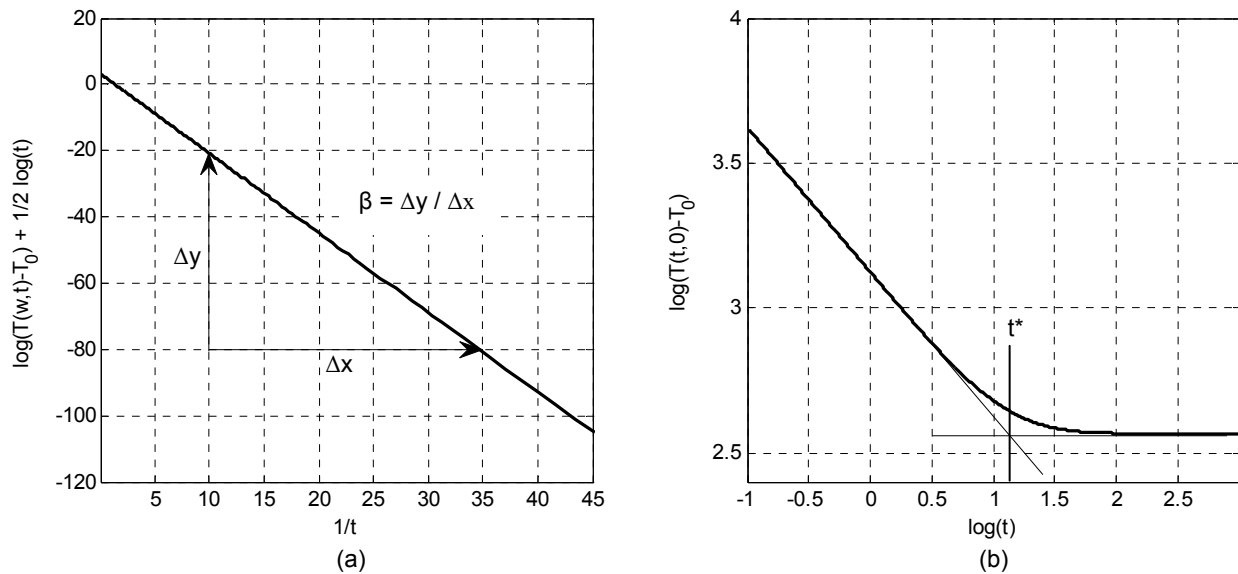


**Fig. 1.** A plot of the temperature evolutions on the back and front surface: (a) linearization of the back surface temperature as used in the LDF algorithm and (b) double logarithmic temperature plot of the front surface as used in the TSR method.

### 3. Finite Element Simulation

In addition to the experiment, numerical simulations of the heat transfer are performed using a FE program. In order to create a model the 2D geometry of the porous CFRP plates is generated from CT measurements (figure 5 – right). This approach enables a simulation of the heat transfer on the basis of real pore morphology. The thermal diffusivity is calculated from the numerically derived temperature field on the front and the back side of the model.

#### 3.1. Model Description

A schematic plot of the 2D FE-model is illustrated in figure 2. The width  $W$  of the model is 20 mm and the thickness  $L$  varies with the porosity content from 4.25 to 5.30 mm. To simulate a pulsed thermographic experiment, the diffusion of heat after a pulse-heating of the surface ( $y = 0$  mm) has been modelled. The pores ( $\Omega_i$ ) are represented as areas with no heat transfer. The basic material ( $\Omega$ ) is simulated using the following thermal properties representing a CFRP plate:  $k = 0.8$  W/(m·K),  $\rho = 1600$  kg/m<sup>3</sup> and  $C_p = 1200$  J/(kg·K) [15].

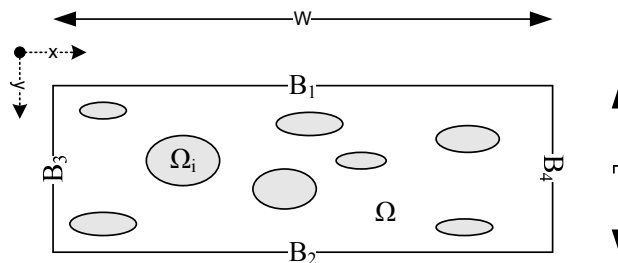


**Fig. 2.** Two-dimensional finite element model with pores.

The mathematical model for the heat transfer by conduction in a 2D geometry is given by following equation

$$\rho C_p \frac{\partial T(t, x, y)}{\partial t} - \nabla \cdot (k \nabla T(t, x, y)) = 0 \quad (7)$$

The boundary conditions for a pulsed thermography experiment are defined as follows

$$k \nabla T|_{B_1} = \begin{cases} q_0 + h(T_0 - T) \rightarrow t \in [t_0, t_p] \\ h(T_0 - T) \rightarrow t \in [t_p, t_{end}] \end{cases}$$

$$k \nabla T|_{B_2} = h(T_0 - T) \quad (8)$$

$$k \nabla T|_{B_3, B_4} = 0$$

The heat flux condition at boundary  $B_1$  represents a heat flux generated from a flash light that enters the material. A pulse duration of  $t_p = 20 \text{ ms}$  and a power per unit of  $q_0 = 5 \cdot 10^5 \text{ W/m}^2$  is used. The convective heat transfer with the surrounding environment at boundary  $B_1$  and  $B_2$  is simulated with a heat transfer coefficient of  $h = 6 \text{ W/(m}\cdot\text{K)}$  and an ambient temperature of  $T_0 = 293 \text{ K}$ . The boundaries  $B_3$  and  $B_4$  are insulated. The initial condition is expressed as follows

$$T(0, x, y) = T_0. \quad (9)$$

For the transient analysis, time steps of 0.1 seconds over a period of 150 seconds are used. The temperature curves are analyzed on 200 points for the front and back side.

### 3.2. Numerical Results

Two numerical results are shown in the case of pores in a carbon-fibre-epoxy matrix with porosity contents of 1.93 % and 4.27 %. For the FE-analyses the rate of porosity is calculated by counting the pixels in the porous phase and dividing the results by the size of the image. The segmented CT cross-section images with an minimum pore size of  $0.02 \text{ mm}^2$  are shown in figure 3a (upper images).

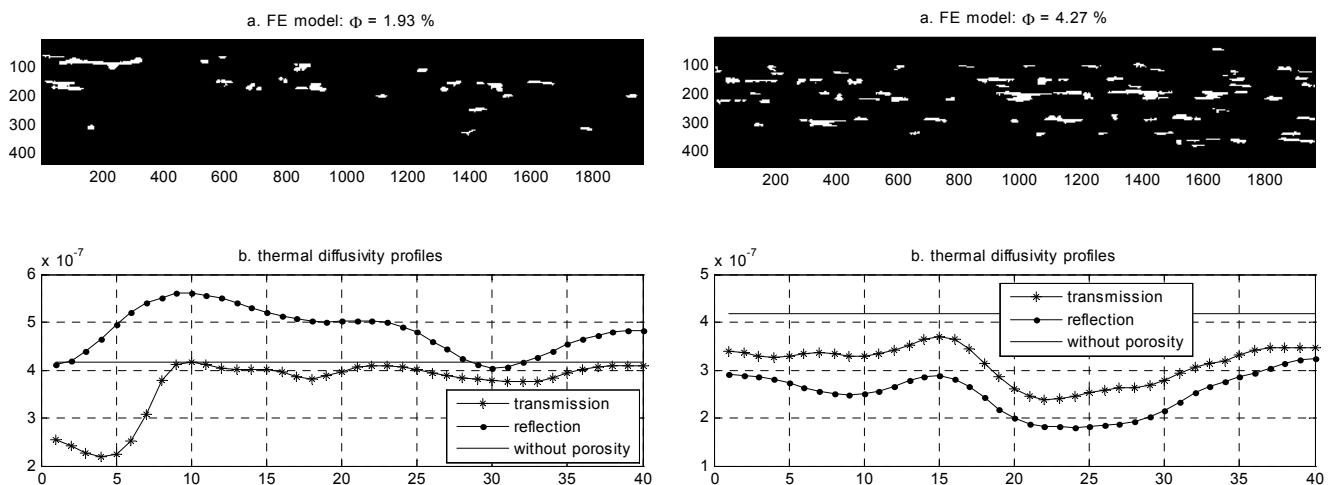


**Fig. 3.** Results of the FE-simulations: a. Geometry of a 2D numerical model with pores and b. thermal diffusivity profiles ( $\text{m}^2/\text{s}$ ) versus the x-coordinate (pixel), calculated from transmission and reflection simulations. Left image shows the model and the diffusivity profiles for a 1.93 % porosity sample, the right images for a 4.27 % porosity sample.

The white areas indicate the pores and the black area the carbon-fibre-epoxy matrix. The numerical calculated transient temperature fields on the front and back are used to determine the effective thermal diffusivity. In figure 3b (lower images) the thermal diffusivities calculated from transmission and reflection results are plotted as a function of the spatial coordinates. In the event that discontinuities are located in the plate, the plotted curves indicate the thermal diffusivity profiles obtained by both transmission and reflection modes. The comparison shows that the reflection results are slightly higher than the transmission results. It has also been observed that where porosity ( $\phi = 1.93\%$  - left images) is low, resulting in inhomogeneous pore distributions, the difference between reflection and transmission results are larger than in samples with a higher amount of porosity ( $\phi = 4.27\%$  - right images). It was also observed that large pores close to the surface have a significant influence on the thermal diffusivity results.

To demonstrate the general dependence of thermal diffusivity on porosity, figure 4 shows averaged thermal diffusivity profile values versus porosity of the FE model. Both the transmission and reflection numerical results indicate that as the total porosity increases, the thermal diffusivity decreases. From the linear behaviour of the transmission results versus porosity, it can be seen that the method is very sensitive with respect to porosity. The scatter seen in the reflection results, especially at low porosity levels, may be due to morphological effects of discontinuities as shown in figure 3b (left). Where porosity levels are above approximately 5% the reflection mode exhibits a lower sensitivity with respect to porosity.

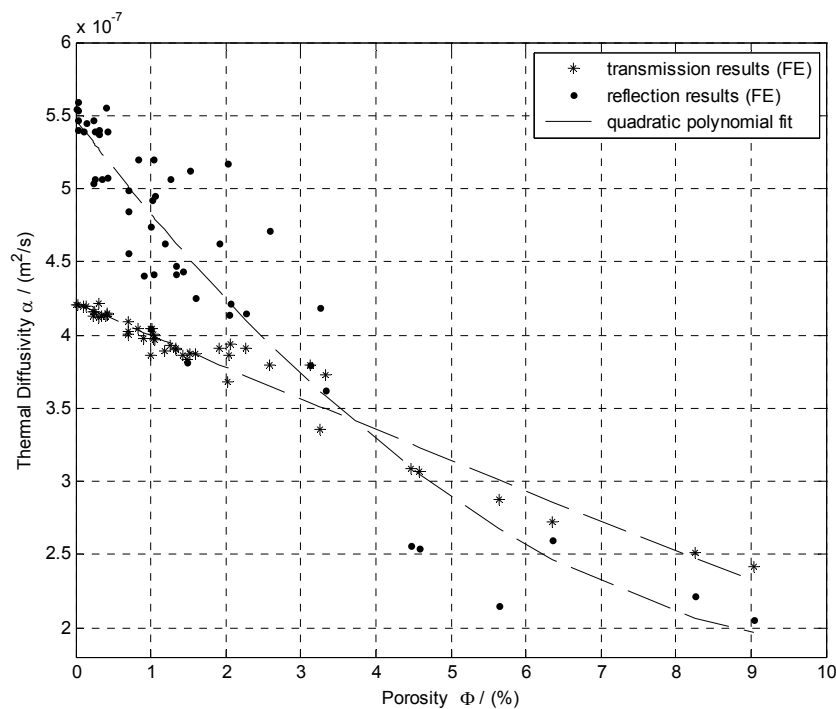


**Fig. 4.** A plot of the effective thermal diffusivity according to FE results and quadratic polynomial fits versus porosity.

## 4. Experiment

### 4.1. Test Specimen

Experiments were performed on nine CFRP plates with thicknesses and porosities given in table 1. The porosities were measured using CT with a spatial resolution of  $(10\ \mu\text{m})^3$ . The samples were made of 20 ply PREPREG C 970/PWC T300 3K UT (TY). The epoxy resin content was 40%. The samples were prepared by changing autoclave parameters, such as temperature and pressure. The specimens were embedded in epoxy resin to reduce edge effects during the experiment. In figure 5, the schematic plot of the test specimen and CT cross-section plots of different porous CFRP specimens are shown.

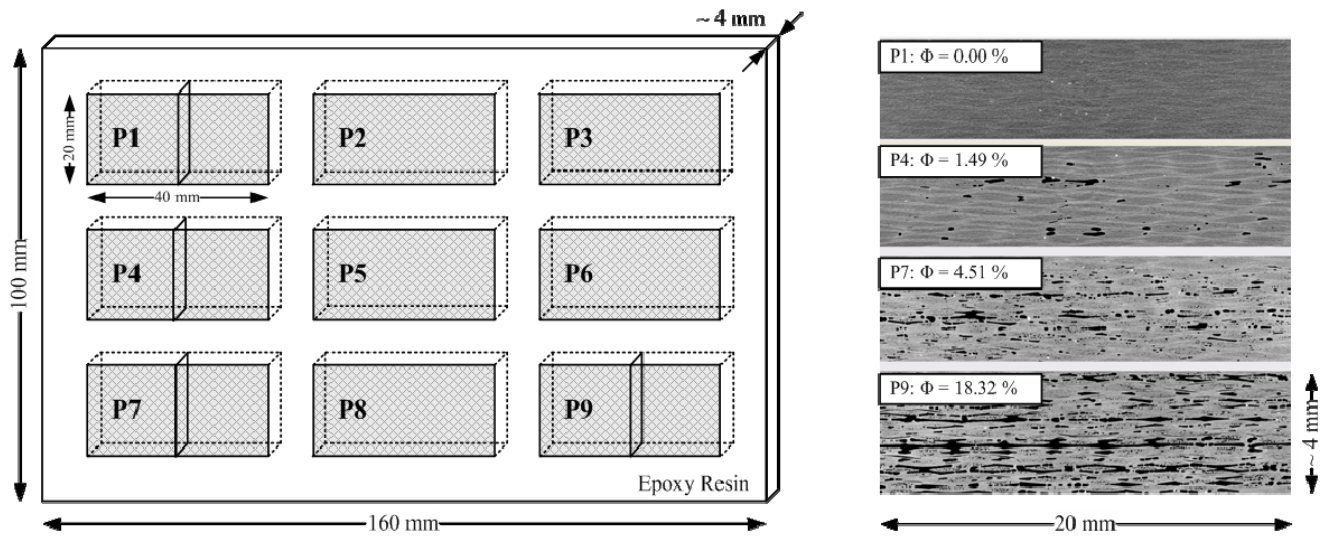


**Fig. 5.** (Left) Epoxy resin test plate with 9 embedded porous CFRP specimens and (right) cross – section plots of different porosity samples generated by CT (the porosity contents represent the average volume porosity over each specimen)

The CT measurements also yield data about the pore diameters which allows a prediction of the homogeneity of the specimen. Kerrisk's criterion of homogeneity (Eq. 2) show that for higher porosity values ( $> 4\%$ ) the material can be considered homogeneously. For lower porosity levels the value  $(d/\Phi^{1/3})$  is up to 2.5 times higher than the upper limit according to Kerrisk (table 1). However, some experts consider this criterion to be unduly restrictive [16] so for low porosity levels the terms of effective thermal diffusivity was used.

**Table 1.** Properties of the CFRP test specimens.

	P1	P2	P3	P4	P5	P6	P7	P8	P9
$L$ (mm)	4.25	4.32	4.35	4.51	4.42	4.50	4.48	4.83	5.30
$\Phi$ (%)	0.00	0.32	0.86	1.49	1.55	4.70	4.51	10.00	18.32
$(d/\Phi^{1/3})/(W/100)$	*	2.45	1.83	1.28	1.43	**	0.92	0.80	**

\* no pores in the specimen, \*\* no geometrical CT data is available

## 4.2. Experimental Setup

The pulsed thermography measurements are performed in reflection mode. The experimental setup consists of an infrared camera (IRCAM Equus 81k M) with a thermal sensitivity of 20 mK in a spectral range of 3 to 5  $\mu\text{m}$ , using a frame rate of 25 Hz. The measurement period was 100 seconds. Two flash lamps with an energy deposition of 6 kJ and pulse duration of approximately 4 ms were used as a source of heat. A standard PC controls the IR camera, acquires and processes the image data.

## 4.3. Experimental Results

The observation time according to Eq. (6) of the CFRP test specimen was measured using the TSR method in reflection mode. The corresponding observation time image is depicted in figure 6. The darkest regions present the lowest values of the observation time  $t_o$  and so exhibit very low porosity. Increased porosity content leads to thicker samples and lower thermal diffusivity values, which accounts for higher observation times.

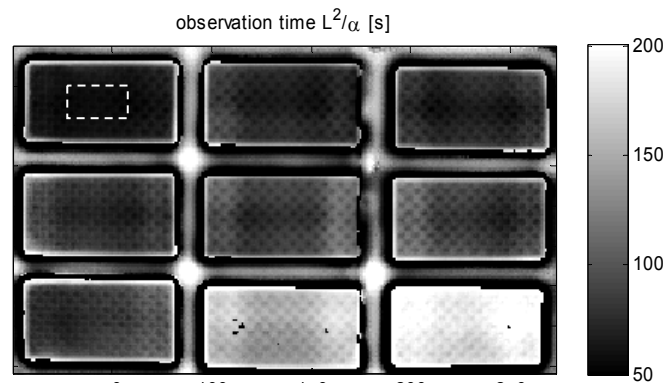


**Fig. 6.** Observation time image of the test specimen with nine different porous CFRP samples.

Only the observation time values of predefined areas (white rectangle in figure 6) with a size of (40 x 20 pixel) are evaluated in order to avoid edge effects. The average value of the observation times in the predefined areas from the sample P1 to P9 are used to calculate the effective thermal diffusivity according to Eq. 6.

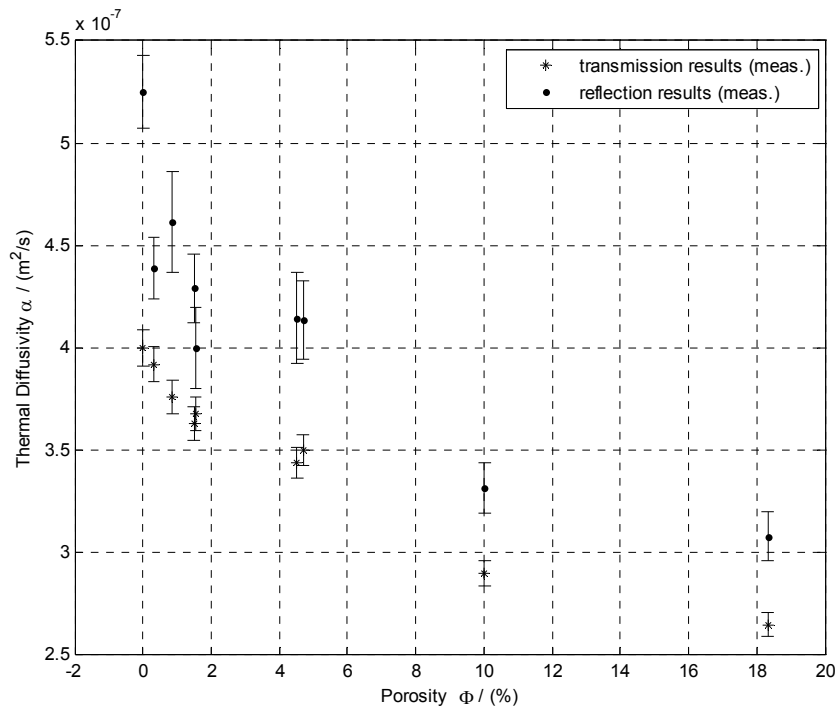


**Fig. 7.** A plot of the effective thermal diffusivity according to pulsed thermography measurements in reflection and transmission mode versus porosity. The transmission results are derived from a former study [10].

The thermal diffusivity as a function of the porosity for the nine test specimens is shown in figure 7. The principal differences of reflection and transmission results are analogous to those seen in the numerical results (figure 4). The results in reflection mode show significantly higher values than in transmission mode. The repeatability was better in transmission measurements than for reflection measurements. Furthermore, at porosity levels higher than 10 % neither the transmission nor the reflection measurements are as sensitive to porosity variations as they are at low porosity levels. This could be due to the increasing tendency of the pores to interlink at higher porosity levels as observed by means of CT.

## 5. Summary

This work successfully demonstrates the combination of pulsed thermography with CT measurements. The volume porosity dependence of the thermal diffusivity is qualitatively shown by 2D numerical simulations and quantitatively by pulsed thermography experiments. The results show that the concept of effective thermal diffusivity can be used for porous CFRP materials to quantify the porosity level. The results of FE analysis show that the effective thermal diffusivity values derived in reflection mode scatters more than those achieved by transmission, especially at low porosity levels. The inhomogeneous spatial pore distribution shows a stronger influence on the reflection than on the transmission results. Furthermore, for porosity levels higher than 10 % the sensitivity of the characterization of porosity decreases for both methods. The presented findings are similar to those seen in the FE analysis. In conclusion, it has been shown that pulsed thermography in reflection mode can also be used to characterize porous CFRP materials with the only drawback being a higher incidence of scatter.

## 6. Acknowledgement

We wish to thank our cooperation partners Eurocopter GmbH and FACC AG as well as FFG (Forschungsförderungsgesellschaft, Austria) for their support within the TAKE OFF project. Furthermore, we thank Christine Peter for her assistance with the FE-analyses. We also wish to acknowledge the help of Jakov Sekelja from FACC for producing samples and Bernhard Plank for the CT tests.

## REFERENCES

- [1] Maldague X.P.V., "Theory and Practice of Infrared Technology for NonDestructive Testing", New York: Wiley-Interscience, 2001.
- [2] Costa, M.L., de Almeida, S.F.M, Rezende, M.C., "The Influence of Porosity on the Interlaminar Shear Strength of Carbon/Epoxy and Carbon/Bismaleimide Fabric Laminates" *Journal of Composite Sciences and Technology*, 61, p. 2101-2108, 2001.
- [3] Judd N.C.W and Wright W.W., "Voids and their effects on the mechanical properties of composites - an appraisal", *SAMPE Journal*, 14(1), p. 10-14, 1978.
- [4] Connolly, M. P., "The Measurement of Porosity in Composite Materials using Infrared Thermography," *Journal of Reinforced Plastic Composites*, 2, p. 1367-1375, 1992.
- [5] Heath D.M. and Winfree W.P., "Thermal Diffusivity Measurement in Carbon-Carbon Composites", *Review of Progress in Quantitative Non-Destructive Evaluation Proceeding*, vol.8B, Thompson D.O., Chimenti D.E. ed., p. 1613-1619, 1989.
- [6] Zalameda, J. N. and Winfree, W. P., "Thermal Diffusivity Measurements on Composite Porosity Samples", *Review of Progress in Quantitative Non-Destructive Evaluation Proceeding*, vol.9, Thompson D.O., Chimenti D.E. ed., p. 1541-1548, 1990.
- [7] Grinzato E., Marinetti S. and Bison P.G., "NDE of porosity in CFRP by multiple thermographic techniques", *Thermosense XXIV Proceeding*, vol.4710, Maldague X.P.V., Rozlosnik A.E. ed., p. 588-598, 2002.
- [8] Ringermacher H.I., Howard D.R. and Gilmore R.S., "Discriminating porosity in composites using thermal depth imaging ", *Review of Progress in Quantitative Non-Destructive Evaluation Proceeding*, vol.21, Thompson D.O., Chimenti D.E. ed., 528-535, 2002.
- [9] Torquato S., "Random Heterogeneous Materials – Microstructure and Macroscopic Properties", New York: Springer, 2002.
- [10] Mayr, G., Hendorfer, G., Plank, B. and Sekelja, J., "Porosity Determination in CFRP Specimens by Means of Pulsed Thermography Combined with Effective Thermal Diffusivity Models", 29<sup>th</sup> *Review of Progress in Quantitative Non-Destructive Evaluation Proceeding*, Kingston (USA), Thompson D.O., Chimenti D.E. ed., 1103-1110, 2010.
- [11] Kerrisk, J.F., "Thermal diffusivity of heterogeneous materials", *Journal of Applied Physics*, 42(1) p. 267-271, 1971.
- [12] Carslaw H.S. and Jaeger J.C., "Conduction of heat in solids", Oxford: University Press, 1959.
- [13] Hendorfer G., Mayr G., Zauner G., Haslhofer M. and Pree R., "Quantitative Determination of Porosity by Active Thermography", 26<sup>th</sup> *Review of Progress in Quantitative Non-Destructive Evaluation Proceeding*, Portland (USA), Thompson D.O., Chimenti D.E. ed., 702-708, 2006.
- [14] Shepard, S.M., "Temporal Noise Reduction, Compression and Analysis of Thermographic Image Data Sequence," US Patent (6,516,084), 2003.
- [15] Maldague X.P.V. and Moore P.O. (editors), "Nondestructive Testing Handbook: Infrared and Thermal Testing", 3<sup>rd</sup> ed., Columbus: ASNT, 2001.
- [16] Lee H.J. and Taylor R.E., "Thermal diffusivity of dispersed composites", *Journal of Applied Physics*, 47(1), p. 148-151, 1976.